Chemico-Biological Interactions 398 (2024) 111094

Contents lists available at ScienceDirect

Chemico-Biological Interactions

journal homepage: www.elsevier.com/locate/chembioint

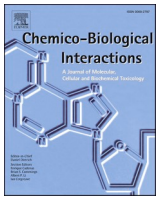

Research paper

Enhancing cisplatin drug sensitivity through PARP3 inhibition: The influence on PDGF and G-coupled signal pathways in cancer

Ayşegül Varol [a], Sabine M. Klauck [b], Françoise Dantzer [c], Thomas Efferth [a,*]

[a] Department of Pharmaceutical Biology, Institute of Pharmaceutical and Biomedical Sciences, Johannes Gutenberg University-Mainz, 55128, Mainz, Germany
[b] Division of Cancer Genome Research, German Cancer Research Center (DKFZ) Heidelberg, National Center for Tumor Diseases (NCT), NCT Heidelberg, a Partnership between DKFZ and University Hospital Heidelberg, 69120, Heidelberg, Germany
[c] Poly(ADP-ribosyl)ation and Genome Integrity, Laboratoire d'Excellence Medalis, UMR7242, Centre Nationale de la Recherche Scientifique/Université de Strasbourg, Institut de Recherche de l'Ecole de Biotechnologie de Strasbourg, 300 bld. S. Brant, CS10413, 67412, Illkirch, France

ARTICLE INFO

Keywords:
Chemotherapy
Drug resistance
Prognostic factors
Signal transduction
Survival analysis
Transcriptomics

ABSTRACT

Drug resistance poses a significant challenge in cancer treatment despite the clinical efficacy of cisplatin. Identifying and targeting biomarkers open new ways to improve therapeutic outcomes. In this study, comprehensive bioinformatic analyses were employed, including a comparative analysis of multiple datasets, to evaluate overall survival and mutation hotspots in 27 base excision repair (BER) genes of more than 7,500 tumors across 23 cancer types.

By using various parameters influencing patient survival, revealing that the overexpression of 15 distinct BER genes, particularly *PARP3*, *NEIL3*, and *TDG*, consistently correlated with poorer survival across multiple factors such as race, gender, and metastasis. Single nucleotide polymorphism (SNP) analyses within protein-coding regions highlighted the potential deleterious effects of mutations on protein structure and function. The investigation of mutation hotspots in BER proteins identified PARP3 due to its high mutation frequency.

Moving from bioinformatics to wet lab experiments, cytotoxic experiments demonstrated that the absence of PARP3 by CRISPR/Cas9-mediated knockdown in MDA-MB-231 breast cancer cells increased drug activity towards cisplatin, carboplatin, and doxorubicin. Pathway analyses indicated the impact of PARP3 absence on the platelet-derived growth factor (PDGF) and G-coupled signal pathways on cisplatin exposure.

PDGF, a critical regulator of various cellular functions, was downregulated in the absence of PARP3, suggesting a role in cancer progression. Moreover, the influence of PARP3 knockdown on G protein-coupled receptors (GPCRs) affects their function in the presence of cisplatin.

In conclusion, the study demonstrated a synthetic lethal interaction between GPCRs, PDGF signaling pathways, and PARP3 gene silencing. PARP3 emerged as a promising target.

1. Introduction

Cellular integrity is under constant threat from exogenous chemicals, physical agents, and endogenous reactive metabolites, leading to the formation of DNA lesions that are toxic and mutagenic [1]. These lesions primarily occur during normal DNA metabolic processes, replication, recombination, and repair. If left unrepaired, they can result in mutations, contributing to age-related diseases and cancer development [2]. To counteract this, cells possess sophisticated defence systems encompassing DNA repair processes, resilience to damage, regulatory checkpoints, and pathways that ultimately govern cellular survival or demise [3,4].

Resistance to cisplatin, a commonly used chemotherapeutic drug, mainly occurs due to increased DNA repair mechanisms, reduced intracellular drug accumulation, and enhanced drug inactivation [5]. To date, a multitude of key biomarkers have been identified that exhibit associations with cisplatin resistance in oncology, as well as poor prognosis and diminished survival outcomes [5]. However, the existing body of literature is characterized by conflicting data, primarily attributable to insufficient and inadequate analyses [5]. Therefore, a comprehensive approach that integrates biomarker expression profiling and polymorphism screening is necessary to accurately determine a patient's resistance status.

Safeguarding against mutagenesis and upholding genome stability relies significantly on the indispensable function of DNA repair

* Corresponding author.
E-mail address: efferth@uni-mainz.de (T. Efferth).

https://doi.org/10.1016/j.cbi.2024.111094
Received 16 February 2024; Received in revised form 7 May 2024; Accepted 31 May 2024
Available online 1 June 2024

Abbreviations

BER	base excision repair
EMT	epithelial-mesenchymal transition
ERK	extracellular signal-regulated kinase
GPCRs	G-protein coupled receptors
IPA	Ingenuity Pathway Analysis software
MAPK	mitogen-activated protein kinase
NF-κB	nuclear factor kappa B-cells
PARP3	poly (ADP-ribose) polymerase 3
PDGF	platelet-derived growth factor
PI3K/Akt	phosphatidylinositol 3 kinase
qPCR	quantitative polymerase chain reaction
ROS	reactive oxygen species
SNP	single nucleotide polymorphisms
TCGA	The Cancer Genome Atlas

mechanisms [3,6]. Among these mechanisms, base excision repair (BER) rectifies minor base alterations induced by oxidation, deamination, and alkylation [7]. BER involves a series of steps, including the removal of base damage, cleavage of the phosphodiester backbone, removal of the sugar-phosphate moiety, and repair completion through short or long patch pathways, depending on the lesion size [8–10]. Although key biomarkers associated with BER proteins have been identified in relation to cisplatin resistance, the exact involvement of BER in drug resistance remains not entirely elucidated [11].

Poly(ADP-ribose) polymerase 3 (PARP3) is a protein intricately involved in BER and has been linked to diverse biological processes, including genome integrity, transcriptional regulation, differentiation, cell metabolism, and cell death [12,13]. PARP3 functions as an activator of PARylation, enhancing PARP1 activity and auto-modification [12, 14]. Its role in transcriptional regulation, chromosomal rearrangements, programmed and stress-induced double-strand break repair, and TGFβ-induced epithelial-mesenchymal transition (EMT) has been established [13,15]. Furthermore, the inhibition of PARP3 function has exhibited potential in curtailing tumor malignancy triggered by mTORC2 signaling, making it a compelling candidate for therapeutic intervention in cancer [16]. However, the exact significance of directing therapeutic efforts towards PARP3 in cancer treatment strategies is yet to be fully understood.

The objective of this study was to investigate alterations in the expression of 27 BER proteins across 23 different cancer types in cancer patients. The study considered parameters such as age, race, gender, metastasis stage, tumor stage, and mutation profile. The primary aim was to predict the most likely target affecting cancer survival and uncover the underlying biological mechanisms. Computational bioinformatics analysis was employed to interpret the genomic data and predict the association between genetic variations and cancer.

Ultimately, the study focused on *PARP3* due to its high expression levels, which correlated with poor survival rates among patients with different parameters, including white race, male gender, and M0 metastasis stage. Furthermore, the association between *PARP3* inhibition and sensitivity to the anticancer drug cisplatin was investigated. The findings demonstrated that inactivating *PARP3* heightened the sensitivity of cancer cells to cisplatin by modulating the G-coupled protein and platelet-derived growth factor (PDGF) signaling pathway. PDGF plays a critical role in various cellular processes, encompassing cell proliferation, transformation, migration, invasion, apoptosis, angiogenesis, and metastasis [17]. Therefore, suppressing PDGF acts as a central regulator of signaling pathways relevant to cancer survival, such as the PI3K/AKT, mTOR, NF-κB, ERK, MAPK, and Notch pathways [17–19]. Targeting the PDGFD receptor signaling pathway is a crucial step in the treatment of cancer patients [20]. Additionally, G-coupled proteins mediate diverse signaling pathways initiated by ligand binding [21]. Identifying selective components that regulate G-protein coupled receptors (GPCRs) may offer novel and effective treatment strategies against cancer [22]. In sum, in this study we endorse the inhibition of *PARP3* to boost the effectiveness of cancer drug therapies by suppressing tumor-promoting actions mediated by GPCRs and PDGF.

2. Material and methods

2.1. Survival analysis

To assess the survival curves associated with the expression of 27 BER genes at the mRNA level, we utilized the Cancer Genome Atlas (TCGA) dataset obtained from cBioportal (https://www.cbioportal.org; accessed between 2020 and 2021) as our primary data source. The TCGA dataset provided comprehensive information on 23 different cancer types, encompassing the expression levels of BER genes, as well as five key parameters: age, race, gender, metastasis, and tumor stage [23]. Subsequently, we conducted Kaplan-Meier survival analyses on each BER gene within the afore-mentioned context.

To determine the statistical significance, we employed the "log-rank" test statistics. By applying this statistical test, we identified survival curves that exhibited noteworthy differences. Specifically, we considered survival curves with a p-value below 0.05 as statistically significant. Subsequently, we compared all the survival curves obtained and focused on the BER gene that demonstrated the highest prevalence in influencing poor patient survival across the five parameters mentioned above.

2.2. Mutation hotspot analysis

To identify mutation hotspots within the coding region of 27 BER proteins, we conducted a comprehensive analysis of mutations across 7,528 patients representing 23 different cancer types [23]. Initially, we employed UniProt, a widely recognized resource for protein information (UniProt, 2023), to determine all the domain sites associated with these proteins. Subsequently, we obtained mutation data from cBioPortal, a valuable platform for exploring cancer genomics data (cBioPortal, 2023) for the years 2020–2021 [23,24]. By examining the mutation profiles of the 27 BER proteins, we identified hotspot sites based on the total number of mutations, irrespective of mutation type. These mutations were categorized as missense, nonsense, or frameshift mutations, allowing us to gain insights into the prevalence and distribution of genetic alterations within this set of proteins. Additionally, we showed the total mutation rate of selected top genes (*PARP3*, *NEIL3*, and *TDG*) in cancer cases.

2.3. Knockout of PARP3 using CRISPR/nCas9-mediated genome editing

Gene knockout of *PARP3* was conducted as previously described [16]. Briefly, cellular transfections into MDA-MB-231 breast cancer cells were carried out with two plasmids, each expressing a pair of guide RNAs (gRNAs) to perform gene knockout experiments. The first plasmid contained gRNAs targeting exon 2 of *PARP3* and co-expressed nCas9-EGFP, while the second plasmid contained gRNAs targeting exon 5 of *PARP3* and co-expressed nCas9-mCherry. Additionally, these plasmids harbored selection cassettes for neomycin or hygromycin resistance, corresponding to the respective gRNA sets. Following transfection, a flow cytometric sorting approach was employed to isolate cells exhibiting co-expression of EGFP and mCherry signals. Subsequently, these cells were cultured for a period of three days in growth media supplemented with hygromycin (350 μg/mL) and G418 (500 μg/mL). Following the selection process, individual colonies were manually picked, expanded, and subjected to genotyping via PCR using primers located upstream of exon 2 and downstream of exon 5 (as mentioned in Ref. [16] before). Subsequently, the PCR products were subjected to sequencing, and the absence of *PARP3* protein in the resulting *PARP3*$^{-/-}$

Table 1
Selected primers for qPCR experiments.

Gene Symbol	Forward Primer	Reverse Primer
PDGFD	CGCCAACCTCAGGCGAGAT	AGAGTGAAGCCGCCATGTCA
MAP2K4	TCCCAATCCTACAGGAGTTCAA	CCAGTGTTGTTCAGGGGAGA
GNB1L	TAGGAGCAGGCGTTCCCGA	CAAACTGGGGGTCTGGAGGT
GPR107	GATGGCGGCCCTTCCTTTCA	ACAACAGCCCAGCCTTCGAT
GPR89A	TCCCAGCAGATAACCTTGCCTC	GCGCATGAAGAAAAGCCACC
GAPDH	TTCGACAGTCAGCCGCATCT	CCGACCTTCACCTTCCCCAT

MDA-MB-231 cells was confirmed through Western blot analysis [16].

2.4. Cytotoxicity assay

The cytotoxicity was assessed employing the resazurin reduction assay, a well-established methodology [25]. This assay facilitates the determination of viable cells based on the reduction of resazurin to resorufin. The impact of carboplatin (ranging from 0.001 μM to 300 μM), as well as doxorubicin and cisplatin (ranging from 0.003 μM to 100 μM) on *PARP3*$^{+/+}$ MDA-MB-231 and *PARP3*$^{-/-}$ MDA-MB-231 cancer cell lines was investigated. The cells were seeded onto 96-well plates. Once they attained approximately 70 %–80 % confluence, the cells were exposed to the specified compounds for a duration of 72 h. Subsequently, the cells were subjected to an additional 4 h incubation period with 20 μL/well of resazurin (Sigma-Aldrich, Germany) diluted in double-distilled water (ddH_2O). The resultant outcomes were recorded using the fluorescence wavelength of 544 nm and an emission wavelength of 590 nm, employing the infinite M2000 ProTM plate reader (Tecan, Germany). The concentrations at which 50 % inhibition occurred (IC_{50}) were calculated using nonlinear regression analysis, utilizing Microsoft Excel.

2.5. Microarray-based expression profiling for predicting canonical pathways

To ascertain the canonical pathway affected by PARP3$^{-/-}$ MDA-MB-231 cells, we conducted microarray hybridization expression analyses. Both the MDA-MB-231 PARP3$^{+/+}$ and PARP3$^{-/-}$ cell lines were subjected to treatment with cisplatin concentrations of 1.6 μM and 0.7 μM, respectively, for a duration of 24 h. Subsequently, total RNA was extracted using the InviTrap® Spin Universal RNA Mini Kit (Invitek Molecular, Berlin, Germany). Following this, complementary DNA (cDNA) was synthesized, labeled, and subjected to hybridization on Affymetrix GeneChips® employing the human Clariom S™ assay (Affymetrix, Santa Clara, CA, USA) at the Genomics and Proteomics Core Facility of the German Cancer Research Center (DKFZ, Heidelberg,

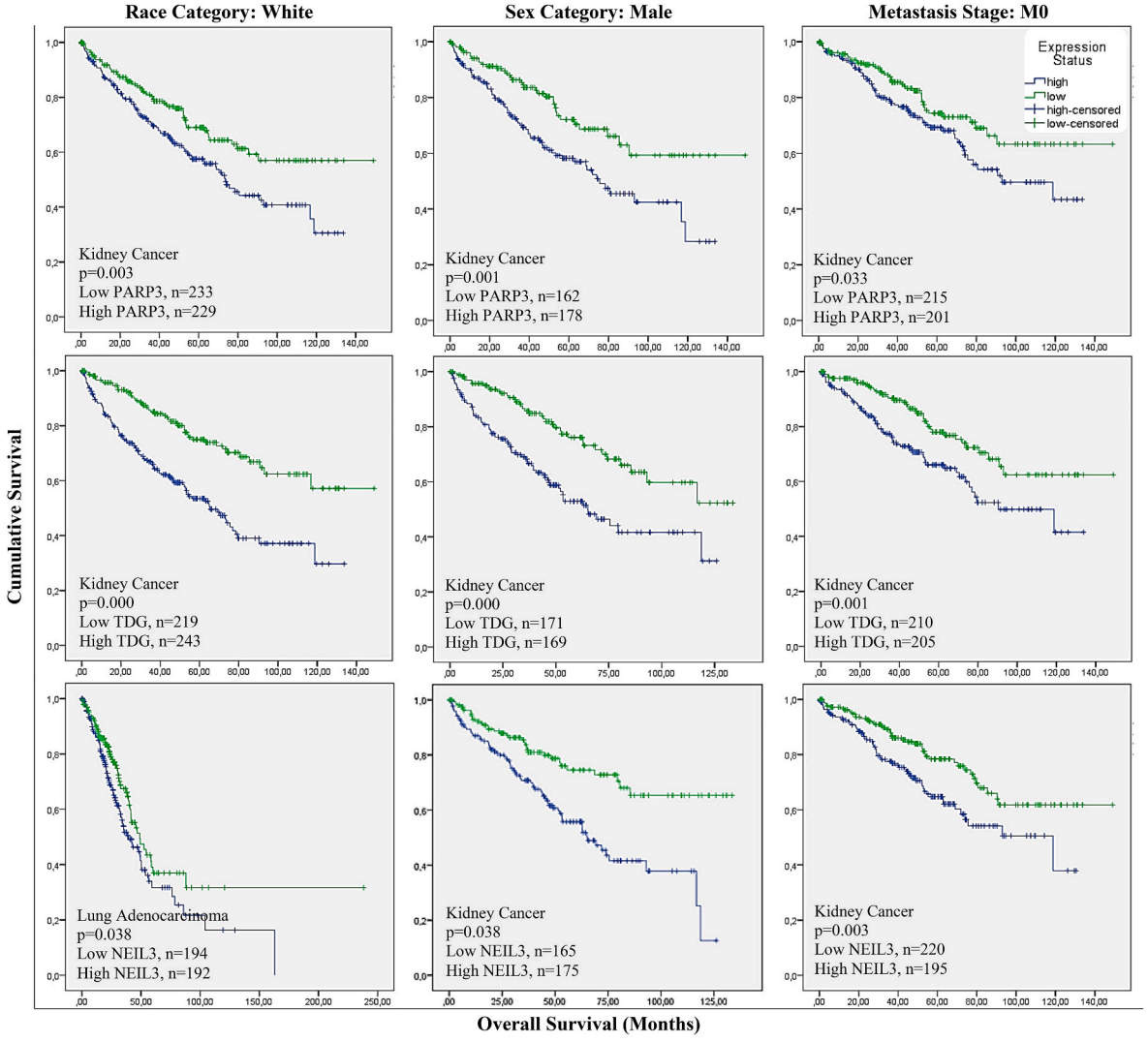

Fig. 1. The association of *PARP3, TDG* and *NEIL3* expression with overall survival of patients (Kaplan-Meier analysis) in kidney renal clear carcinoma and lung adenocarcinoma.

Table 2
The mutational hotspot sites and the mutation frequency of 27 base excision repair genes.

Gene	Missense	Nonsense	Frameshift	Hotspot domain	Total mutation number
LIG3	17	4	2	DNA ligase N terminus (261–435)	23
TDP1	25	1	1	Tyrosyl-DNA phosphodiesterase (163–582)	27
TDP2	16	2	4	Endonuclease/exonuclease/phosphatase family (117–351)	22
SMUG1	15	3	1	Uracil DNA glycosylase (71–262)	19
HUS1	15	2	2	HUS1 (1–280)	19
RAD9A	14	–	4	Rad9 (13–265)	18
PARP1	18	–	–	PARP polymerase catalytic (788–1014)	18
PARP3	16	1	–	PARP catalytic (313–533)	17
APEX1	13	1	3	Endonuclease/exonuclease/phosphatase (65–309)	17
NEIL1	9	2	6	Formamidopyrimidine-DNA glycosylase N-terminal domain (2–123)	17
TDG	15	1	–	Uracil DNA glycosylase (139–300)	16
LIG1	15	1	–	DNA ligase N terminus (287–465)	16
MPG	14	1	1	Methylpurine-DNA glycosylase (139–300)	16
UNG	13	1	1	Uracil DNA glycosylase (139–300)	15
RAD1	12	2	1	Rad1 (16–257)	15
NEIL3	9	–	5	GRF zinc finger (506–548) (552–595)	14
MUTYH	12	–	1	Nudix hydrolase (364–495)	13
PARP2	10	1	2	PARP catalytic (356–583)	13
NEIL2	11	–	1	Formamidopyrimidine-DNA glycosylase N-terminal domain (2–180)	12
NUDT1	7	2	1	Nudix hydrolase (45–168)	10
XRCC1	8	1	1	BRCT1 (315–403)	10
NTHL1	9	–	1	HhH-GPD (135–271)	10
PCNA	7	1	–	PCNA C terminal (127–254)	8
PNKP	7	1	–	Polynucleotide kinase 3 phosphatase (166–328)	8
OGG1	7	–	–	8-oxoguanine DNA glycosylase (25–141)	7
FEN1	6	–	1	I-domain (122–253)	7
MBD4	4	1	–	Methyl-CpG binding domain (80–149)	5

Germany). The affected genes were then observed utilizing Chipster software (version 3.16.3) (accessed on 21 June 2020), whereby their variable expression and significance were evaluated based on the empirical Bayes *t*-test ($p < 0.05$).

To demonstrate the canonical pathway affected by *PARP3* inhibition, we employed Ingenuity Pathway Analysis software (IPA; Ingenuity Systems, Redwood City, CA, USA), utilizing the content version 51963813, released on 01/01/2023. IPA facilitated the assessment of changes in canonical pathways between the $PARP3^{+/+}$ and $PARP3^{-/-}$ MDA-MB-231 cancer cell lines following cisplatin exposure. To compare the effects of cisplatin exposure on $PARP3^{+/+}$ and $PARP3^{-/-}$ MDA-MB-231 cells, gene heatmaps and canonical pathway analyses were conducted, employing activation z-scores and *p*-values as metrics.

2.6. Quantitative real-time qPCR for validating relative gene expression

After identifying the canonical pathway associated with the absence of *PARP3*, we proceeded to validate the microarray findings through the utilization of qPCR technique. Primers were designed using the Primer BLAST online tool (https://www.ncbi.nlm.nih.gov/tools/primer-blast/) (accessed in 2023) and procured from Eurofins Genomics (Ebersberg, Germany). The selected primers are presented in Table 1 for selected signaling pathway and Supplementary Table S2. Subsequently, qPCR was performed on the selected genes. Briefly, the MDA-MB-231 wild-type and MDA-MB-231 *PARP3* knockout cancer cells were treated with cisplatin concentrations equivalent to their respective IC_{50} values, specifically 1.6 μM and 0.7 μM, for a duration of 24 h. Total RNA extraction was carried out using the InviTrap® Spin Universal RNA Mini Kit (Invitek Molecular, Berlin, Germany). The conversion from mRNA to cDNA was accomplished utilizing the LunaScript® RT SuperMix Kit cDNA Synthesis Kit (New England Bio Labs, Darmstadt, Germany). Subsequently, gene amplification was performed using the EvaGreen master mix (5 × Hot Start Taq EvaGreen® qPCR Mix (no ROX); Axon Labortechnik, Kaiserslautern, Germany) according to the manufacturer's instructions.

Real-time PCR was conducted on a CFX384TM instrument (Bio-Rad, Munich, Germany) using a 38-well plate and employing 40 cycles. The run conditions consisted of three steps: an initial denaturation phase at 95 °C for 15 s, followed by a gradient annealing step ranging from 62 °C to 47 °C for 30 s, and finally, an elongation step at 72 °C for 1 min. To determine the fold-change in gene expression, the comparative Cq ($2^{-\Delta\Delta Cq}$) method was employed [26].

2.7. Single cell gel electrophoresis (comet assay)

The comet assay was conducted utilizing the Oxiselect™ Comet Assay Kit (3-Well Slides) sourced from Cell Biolabs/Biocat in Heidelberg, Germany. Initially, $PARP3^{+/+}$ and $PARP3^{-/-}$ MDA-MB-231 cells were seeded at a density of 1×10^6 cells per well in 6-well plates. Subsequently, these cells were subjected to treatment with cisplatin concentrations corresponding to their respective IC_{50} values, specifically 1.6 μM and 0.7 μM, over a period of 24 h. Additionally, H_2O_2 at a concentration of 50 μM was applied as a positive control for a duration of 15 h.

Following treatment, the cells were collected, subjected to centrifugation at 3000×*g* for 10 min, and then reconstituted in PBS. Subsequently, cell suspensions at a concentration of 1×10^5 cells/mL were blended with molten agarose at 37 °C at a ratio of 1:6. The resulting mixtures were then evenly spread onto comet slides and allowed to incubate in darkness at 4 °C for 30 min. The slides were subsequently immersed in a pre-chilled lysis buffer (comprising of 14.6 g NaCl, 20 mL EDTA solution, and 10 × lysis solution at pH 10.0) for a duration of 1 h at 4 °C in darkness. Post-lysis, the slides were withdrawn from the lysis buffer and immersed in a pre-chilled alkaline electrophoresis solution buffer (consisting of 12 g NaOH, 2 mL EDTA solution, and 1000 mL distilled water) for 40 min at 4 °C in darkness. The slides were then placed into an electrophoresis chamber filled with the afore-mentioned alkaline electrophoresis solution buffer, and electrophoresis was conducted at 20 V for 20 min. Subsequently, the slides underwent two washes with prechilled distilled water, each for 5 min. Following the washes, the slides were immersed in cold ethanol (70 %) for 5 min, after which they were allowed to air-dry. Upon complete desiccation, 100 μL of Vista Green DNA dye, diluted at a ratio of 1:10,000 in TE buffer (comprising of 10 mM Tris and 1 mM EDTA at pH 7.5), was added to each slide and permitted to incubate for 15 min at room temperature. Subsequently, 50 comets from each treatment group were randomly

Table 3
The prevalence of genetic modifications in *PARP3, TDG*, and *NEIL3* across specific cancer types investigated by The Cancer Genome Atlas (TCGA) was examined using the cBioPortal database to analyze the distribution of gene alterations.

Cancer type	Total number of cases	Cases with altered genes (%)		
		PARP3	*TDG*	*NEIL3*
Breast invasive cancer	963	9 (0.9)	5 (0.5)	18 (1.9)
Glioblastoma multiforma	273	1 (0.4)	3 (1.1)	2 (0.7)
Colorectal adenocarcinoma	220	1 (0.5)	2 (0.9)	8 (4)
Esophageal carcinoma	184	6 (3)	3 (1.6)	9 (5)
Stomach adenocarcinoma	441	13 (2.9)	9 (2)	20 (5)
Head and neck squamous cell carcinoma	504	6 (1.2)	3 (0.6)	17 (3)
Kidney renal clear cell carcinoma	448	52 (12)	1 (0.2)	1 (0.2)
Liver hepatocellular carcinoma	366	4 (1.1)	7 (1.9)	12 (3)
Lung adenocarcinoma	230	1 (0.6)	3 (1.7)	12 (7)
Pancreatic adenocarcinoma	149	–	2 (1.3)	2 (1.3)
Prostate adenocarcinoma	492	5 (1)	8 (1.6)	8 (1.6)
Skin cutaneous melanoma	287	4 (1.4)	5 (1.7)	8 (2.8)
Thyroid carcinoma	399	–	–	1 (0.3)
Ovarian cancer	311	4 (1.3)	7 (2.3)	17 (5)
Uterine corpus endometrial carcinoma	56	–	–	1 (1.8)
Bladder urothelial carcinoma	127	5 (4)	2 (1.6)	5 (4)
Cervical cancer	191	4 (2.1)	–	6 (3)
Sarcoma	243	5 (2.1)	5 (2.1)	7 (2.9)
Testicular	149	1 (0.7)	–	1 (0.7)
Thymoma	123	–	–	1 (0.8)
Pediatric acut lymphoid leukemia	95	–	–	5(%5)
Pediatric neuroblastoma	1089	–	–	1(% 0.1)

selected and subjected to analysis via OpenComet, a software tool integrated within Image J, developed by the National Institutes of Health. Tail DNA% was employed as the parameter for quantifying DNA damage [27].

3. Results

3.1. Survival analysis

First and foremost, we have identified the target gene that is most frequently associated with poor survival across five parameters in 23 different cancer types. In order to identify the target gene specifically related to survival, we thoroughly examined the results obtained from the five parameters age, race, gender, metastasis stage, and tumor stage. Our scrutiny involved an in-depth analysis of survival curves derived from the expression patterns of 27 genes involved in the BER pathway. Notably, statistically significant survival curves were discerned for 15 genes within the BER pathway. Furthermore, it is noteworthy that no statistically significant survival curves were observed in relation to age and tumor stage, as elucidated in Fig. 1, Supplementary Table S1, and Supplementary Fig. S1.

Subsequently, we conducted a comparative analysis to determine the most commonly observed protein in terms of survival curves across different categories. Based on the survival curves, we revealed that high expression levels of *PARP3*, *TDG*, and *NEIL3* had a significant impact on cancer survival. This impact was particularly notable in three distinct categories: race, gender, and metastasis stage. In contrast, the remaining BER gene expressions were observed in fewer than three categories.

Specifically, in kidney renal clear carcinoma cancer, the high expression of *PARP3* and *TDG* was associated with decreased overall patient survival in the white race, male patient group and M0 metastasis stage. Furthermore, high expression of *NEIL3* resulted in poor survival among the white race in both lung adenocarcinoma and kidney cancers, as well as in the male patient group and M0 metastasis stage and in kidney cancer types (Fig. 1).

3.2. Determination of mutation hotspots

For identification of most probable predictive target, our investigation primarily concentrated on missense, nonsense, and frameshift mutations, aiming to determine mutation hotspot sites based on the existing mutation data across 23 different cancer types. Initially, we exhaustively examined all domain sites associated with the 27 BER genes and subsequently identified the hotspots exhibiting the highest mutation frequencies. These mutation hotspot domain sites across the 27 BER genes are visually represented in Table 2. Additionally, total mutation rates of selected genes in the different cancer types are shown in Table 3. Considering the outcomes of our survival analyses, we prioritized the gene with the highest mutation frequency. Consequently, we conducted further analyses specifically focusing on *PARP3* to gain a comprehensive understanding of its impact on cancer survival. The rationale behind this choice is rooted in the fact that *PARP3* exhibited the highest mutation frequency among the selected three genes, as observed through the consequences of the survival analyses. The mutation profiles of *PARP3, TDG*, and *NEIL3* are shown in Table 3 and Fig. 2.

3.3. Cytotoxicity assay

The cytotoxicity assay to assess cell viability was conducted using cisplatin, carboplatin, and doxorubicin, and a comparison was made between the $PARP3^{+/+}$ MDA-MB-231 cell line and the $PARP^{-/-}$ MDA-MB-231 cells. The *PARP3* knockout MDA-MB-231 cells exhibited diminished growth compared to the wild-type cells in response to the three drugs after 72 h. Interestingly, the absence of *PARP3* appeared to enhance the efficacy of cisplatin, carboplatin, and doxorubicin.

Specifically, the $PARP3^{-/-}$ MDA-MB-231 cells demonstrated a 50 % inhibition of cell viability (IC_{50}) at a cisplatin concentration of $0.7 \pm < 0.01$ μM, a carboplatin concentration of 2.2 ± 0.7 μM, and a doxorubicin concentration of $0.2 \pm < 0.01$ μM. In contrast, $PARP3^{+/+}$ MDA-MB-231 cell exhibited a IC_{50} value at a cisplatin concentration of 1.6 ± 0.15 μM, a carboplatin concentration of 8 ± 0.57 μM, and a doxorubicin concentration of 0.4 ± 0.03 μM (Fig. 3). These findings indicate that the $PARP3^{-/-}$ MDA-MB-231 cell line was sensitized to the cytotoxic effects of cisplatin, carboplatin, and doxorubicin, leading to a significant reduction in cell viability.

3.4. Microarray-based mRNA expression profiling for predicting canonical pathways

Upon identification of the most probable target genes based on the overall survival analyses and mutation profiles in 23 types of cancer, we proceeded to perform a microarray analysis with the objective of examining the consequences of *PARP3* inhibition as a target for cancer drug therapy. Subsequently, we compared two groups, namely the $PARP3^{+/+}$ and $PARP3^{-/-}$ MDA-MB-231 cell lines, following exposure to cisplatin, in order to unveil the mechanisms associated with *PARP3* through comparative analysis using Ingenuity Pathway Analysis (IPA). The data obtained revealed a significant impact of *PARP3* inhibition on signal pathways implicated in cancer cell survival.

The data derived from this analysis divulged that the inhibition of

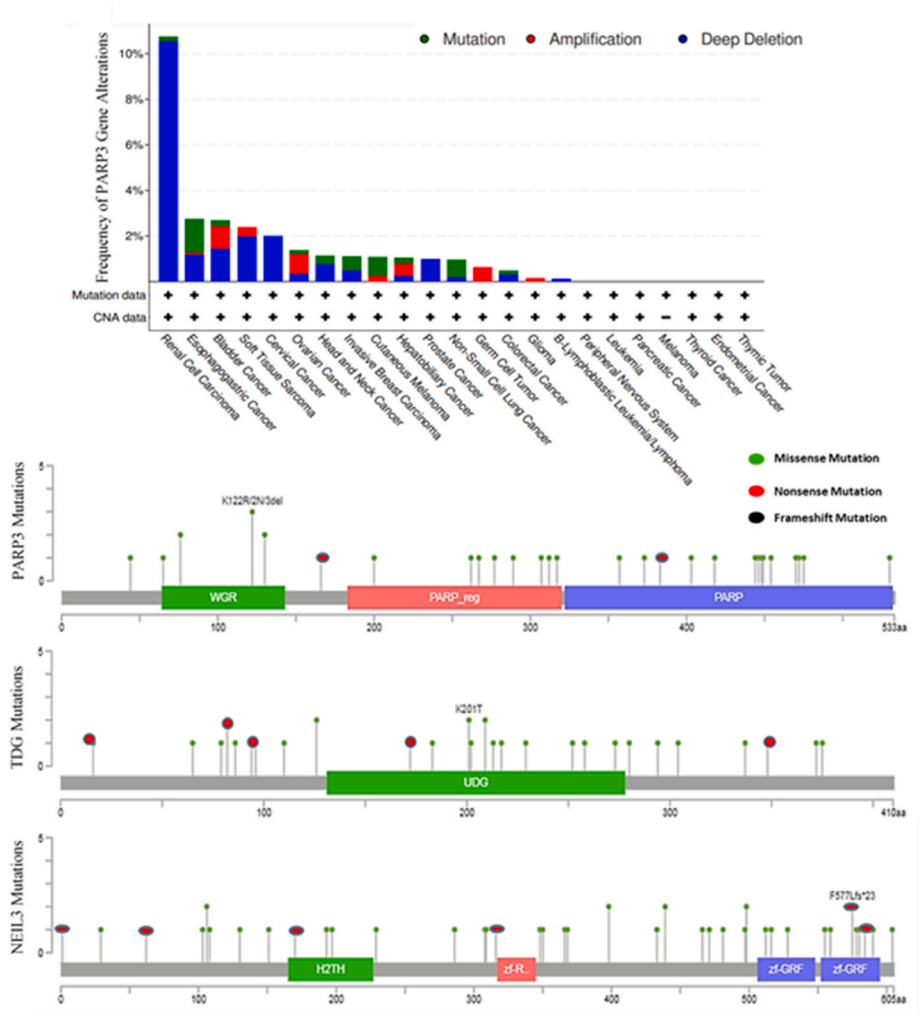

Fig. 2. Frequency of *PARP3* gene modifications in the specified cancer cases, alongside the distribution of mutation profiles associated with *PARP3*, *TDG*, and *NEIL3*.

PARP3 exerts a significant impact on signal pathways that decrease the survival of cancer cells. Specifically, in the *PARP3*$^{+/+}$ MDA-MB-231 cell line, following exposure to cisplatin, signal pathways closely associated with cellular growth and proliferation remained active, as depicted in Fig. 4. Notably, upon scrutinizing the canonical pathway of *PARP3*$^{+/+}$ MDA-MB-231, PDGF and GPCRs emerged as the most prominently active signaling cascades. Remarkably, both PDGF and GPCRs pathways exhibited highly positive z-scores, registering at 2.4 and 2.236, respectively. Consequently, we directed our focus towards these two crucial signal pathways.

However, it is worth noting that these afore-mentioned pathways (*i.e.*, GPCR and PDGF) did not exhibit activation in the *PARP3*$^{-/-}$ MDA-MB-231 cell line following exposure to cisplatin. Instead, the absence of *PARP3* led to a decrease in the activation of EIF2 and protein kinase A signaling. On the other side, upon examining the canonical pathways, we observed the activation of the oxytocin signal, the apelin endothelial signal, and the m-TOR signal pathway due to the influence of the GPCR and PDGF pathways in the *PARP3*$^{+/+}$ MDA-MB-231 cell lines.

3.5. Quantitative real-time qPCR for validating relative gene expression

To validate the findings from the microarray analyses, quantitative polymerase chain reaction (qPCR) experiments were performed. Pathway analysis was conducted to investigate whether the absence of *PARP3* in the context of cisplatin treatment impacted the PDGF and GPCR canonical pathways. For this analysis, we selected specific genes, namely *PDGFD*, *MAP2K4, GNB1L, GP107*, and *GPR89A* which are known to be involved in the PDGF and GPCR signaling pathways. The selected primers demonstrated a downregulation of gene expression in the presence of *PARP3* inhibition in the cell line exposed to cisplatin. Conversely, the expression of all genes investigated were upregulated in the *PARP3*$^{+/+}$ MDA-MB-231 cell line following cisplatin treatment (Fig. 5C). This finding was consistent with the results obtained from the microarray analyses (Fig. 5A), reinforcing the concordance between the two experimental approaches.

3.6. Single cell gel electrophoresis (comet assay)

In order to evaluate DNA damage in MDA-MB-231 cell lines devoid of *PARP3*, we utilized the alkaline comet assay as a means of detection. Our investigation revealed a noteworthy elevation in DNA damage within the *PARP3*$^{-/-}$ MDA-MB-231 cell line if exposed to a cisplatin concentration of 0.7 μM. Conversely, under the application of a higher cisplatin concentration (1.6 μM) in the wild-type cell line, the percentage of comets decreased and, therefore, less DNA damage was observed (Fig. 6). This discernible discrepancy suggests that the lack of *PARP3* renders the cells more susceptible to lower concentrations of cisplatin.

4. Discussion

Drug resistance represents a pervasive phenomenon encountered in cancer treatment, particularly in the context of platinum-based drugs

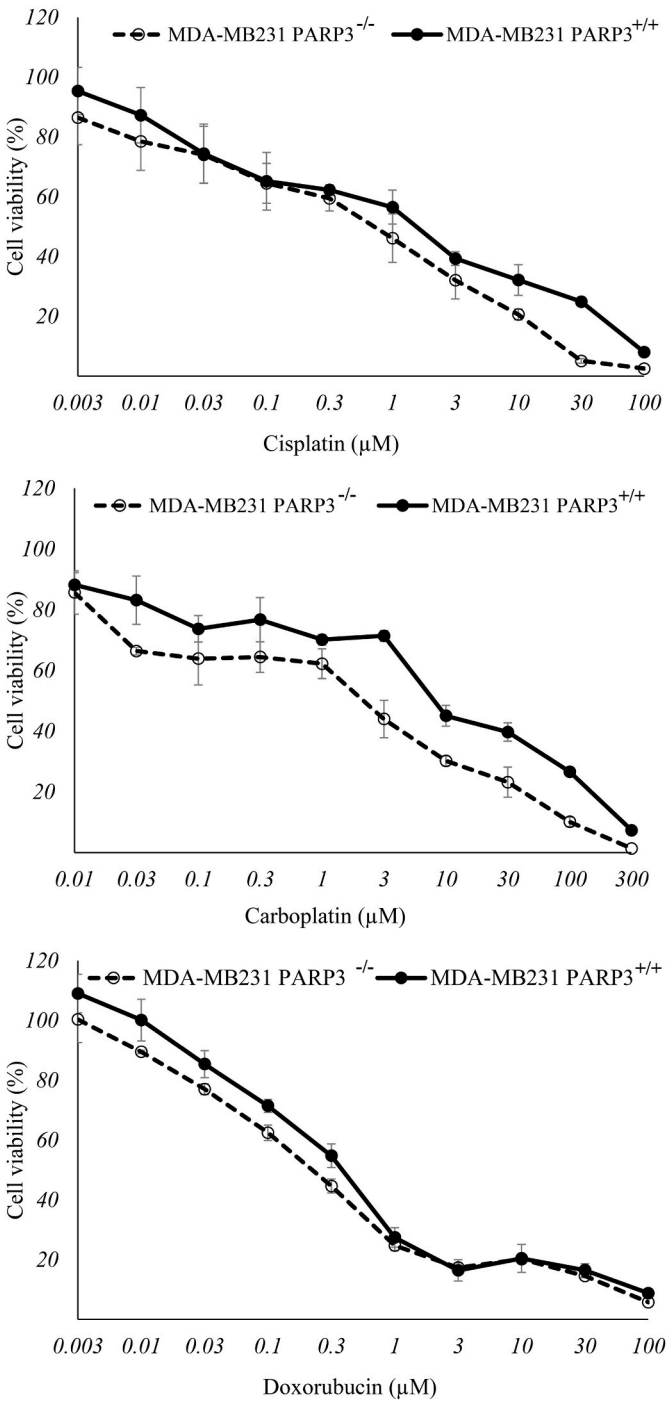

Fig. 3. Growth inhibition of *PARP3*$^{+/+}$ and *PARP3*$^{-/-}$ MDA-MB-231 cell lines for cisplatin, carboplatin, and doxorubicin by using the resazurin reduction assay.

such as cisplatin [5,28]. The primary factor underlying the development of cisplatin resistance lies in the compromised cellular uptake of the drug, the perturbation of DNA repair mechanisms, diminished cell death signaling, and augmented drug inactivation [29,30]. Despite cisplatin's substantial clinical efficacy across various cancer types, the emergence of drug resistance continues to impede patient survival and therapeutic efficacy [30]. Evidently, the identification and targeting of key molecular pathways associated with drug resistance hold significant promise in enhancing drug activity and improving clinical outcomes for patients [5]. The accurate prediction of appropriate biomarkers can be facilitated through the utilization of comprehensive bioinformatics analysis. Consequently, we employed a comparative analysis of multiple datasets in this study. By evaluating the overall survival and identifying mutation hotspots in 27 BER genes across 23 cancer types, encompassing a cohort of 7,528 patient samples, we successfully identified the most probable predictive targets.

Overall survival is known as a parameter denoting the duration between a patient's entry into a clinical trial and their demise from any cause [31,32]. Analyzing the overall survival times allows the assessment of treatment outcomes [33,34], cancer-specific biomarkers [35], as well as biological or other interventions within the realm of oncological clinical trials [36]. Patient survival is influenced by various factors, including age, race, gender, and lifestyle choices [37]. Identifying the factors that contribute to increased overall survival time is crucial for expediting the development of novel and efficacious therapies. Moreover, considering multiple factors not only helps prevent conflicting data but also aids in identifying the most probable target associated with overall survival. Undoubtedly, employing novel multiple data models is imperative for selecting a target linked to patients' survival [38]. In the present study, we compared five parameters to identify the most likely target impacting patient survival. Ultimately, we observed that the overexpression of 15 distinct BER genes under various parameters led to poorer survival outcomes (provided as Supplementary File). *PARP3*, *NEIL3*, and *TDG* emerged as the most compelling targets, as the high expression of all three BER genes was consistently associated with poorer survival across three out of the five parameters assessed, which encompassed race, gender, and metastasis stage.

Up to now, high expression of *PARP3*, *NEIL3* and *TDG* have been found to be related to poor prognostic outcomes [39–41]. Especially, the high expression of genes involved in DNA repair were directly correlated with increasing drug sensitivity and cancer progression [42]. Thus, the inhibition of DNA repair is accepted as means to increase anticancer agents' sensitivity [43]. In contrast, the downregulation of these genes are likely to exhibit a reduced DNA repair activity, leading to the accumulation of mutations [44]. Obviously, mutated genes may lead to the loss of the nuclear expression of the corresponding proteins. However, there are numerous other factors affecting protein expression, including the level of transcription, splicing, the stability of mRNA, posttranslational modifications, and epigenetic factors [45].

In addition to the analysis of survival curves, we conducted a comparative analysis in terms of single nucleotide polymorphisms (SNPs). SNPs occurring within protein-coding regions have garnered significant attention within the scientific community, despite the fact that these regions account for only approximately 2 % of the total human genome [46]. The rationale behind this attention stems from the potential deleterious effects resulting from mutations within protein cores, which can lead to protein misfolding or alterations in protein translation [47]. Furthermore, these mutations can impact gene expression levels in two distinct ways: by modifying gene dosage through changes in the number of gene copies, or by affecting gene regulation [48]. Generally, missense mutations have the potential to influence protein expression levels, hinder protein function, or directly impact drug-binding affinities, while nonsense mutations result in the truncation of proteins [46,48]. In addition to missense and nonsense mutations, frameshift mutations pose a greater likelihood of causing more severe phenotypic effects. This is due to their propensity to cause extensive alterations in the nucleotide sequence, resulting in either silent mutations or conservative changes in protein products [49]. It is evident that point mutations lead to structural modifications in proteins, which can potentially impact gene network interactions. These alterations may include changes in binding affinity towards natural partners, as well as impairment in interactions with ligands and/or inhibitors [46]. The presence of such point mutations can disrupt protein function, leading to the development of drug resistance. Therefore, evaluating the mutation status offers valuable insights into the correlation between resistance and structural alterations in proteins, shedding light on the underlying mechanisms. Following the identification of the most

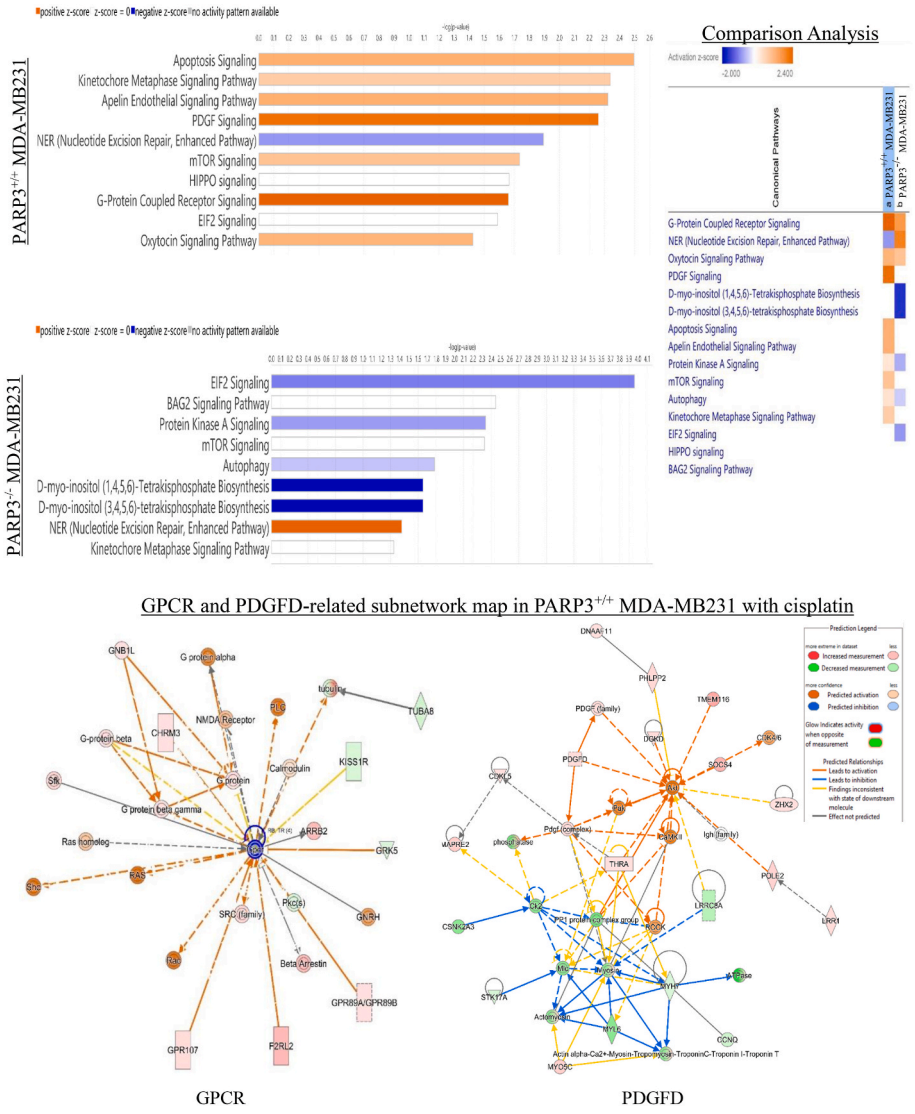

Fig. 4. Comparison of canonical pathways in *PARP3* wild-type and knockout MDA-MB-231 cells, following cisplatin exposure. The figure includes a comparative analysis of the canonical pathways between the two groups, with a specific focus on the subnetwork map of G-coupled protein receptor and PDGFD-related molecules in *PARP3* wild-type cells treated with cisplatin.

promising targets through survival analysis, we compared the mutation hotspots of 27 BER proteins across 23 cancer types. Consequently, we concentrated on *PARP3* due to its highest mutation frequency.

Cisplatin affects cancer cells by binding to specific sites in the DNA, *e.g.*, by binding to the N-7 positions of adenine and guanine [50]. These binding interactions result in the formation of interstrand and intra-strand crosslinks which impair DNA structure and DNA functions, including replication and transcription [51], leading to retarded cell growth and induction of cell death [52]. However, changes in the DNA binding sites due to mutations can alter cisplatin's ability to bind to DNA turning the expression of specific genes on or off and, thereby, resulting in non-desired changes in protein expression. This can increase toxicity to normal cells or lead to drug resistance in cancer cells. The application of combination therapies represents a common approach to dampen side effects of cisplatin on normal tissues and enhance cisplatin sensitivity towards tumor cells caused by cisplatin-caused DNA mutations. On the other hand, the identification of unwanted gene expression by computational methods, such as molecular docking, molecular dynamic, and machine learning, as well as experimental techniques may enable to design novel effective target-specific ligands as novel partners for cisplatin-based combination regimens in the future [46]. Another aspect in this context is the appearance of SNPs that also affect cisplatin-induced cytotoxicity by influencing gene expression [53]. In addition, integrated "-omics" analyses may considerably facilitate the identification of cisplatin-induced off-target effects, which may pave the way for gene-editing tools specifically targeting cancer cells and simultaneously sparing normal cells. Moreover, improvement drug delivery systems could reduce adverse effects of cisplatin by targeting only cancer cells [54].

Experimental determination of differences between mutant and wild-type proteins represents a fundamental step in understanding the influence of protein expression and variations [46]. Therefore, we conducted cytotoxic experiments to observe the consequences of *PARP3* inhibition in the presence of cisplatin. According to our microarray results, the increased expression of gene involved in nucleotide excision repair (NER) was caused from the inhibition of BER. Obviously, cells have multiple mechanisms to maintain genomic stability. If one mechanism is interrupted, another alternative mechanism may take over the protection of cellular integrity. It is apparent that there are more than 20 genes involved in BER genes, each performing a unique function. Obviously, each of them has distinct connections with the other neighbourhood genes. Our studies focussed only on the impact of *PARP3* on

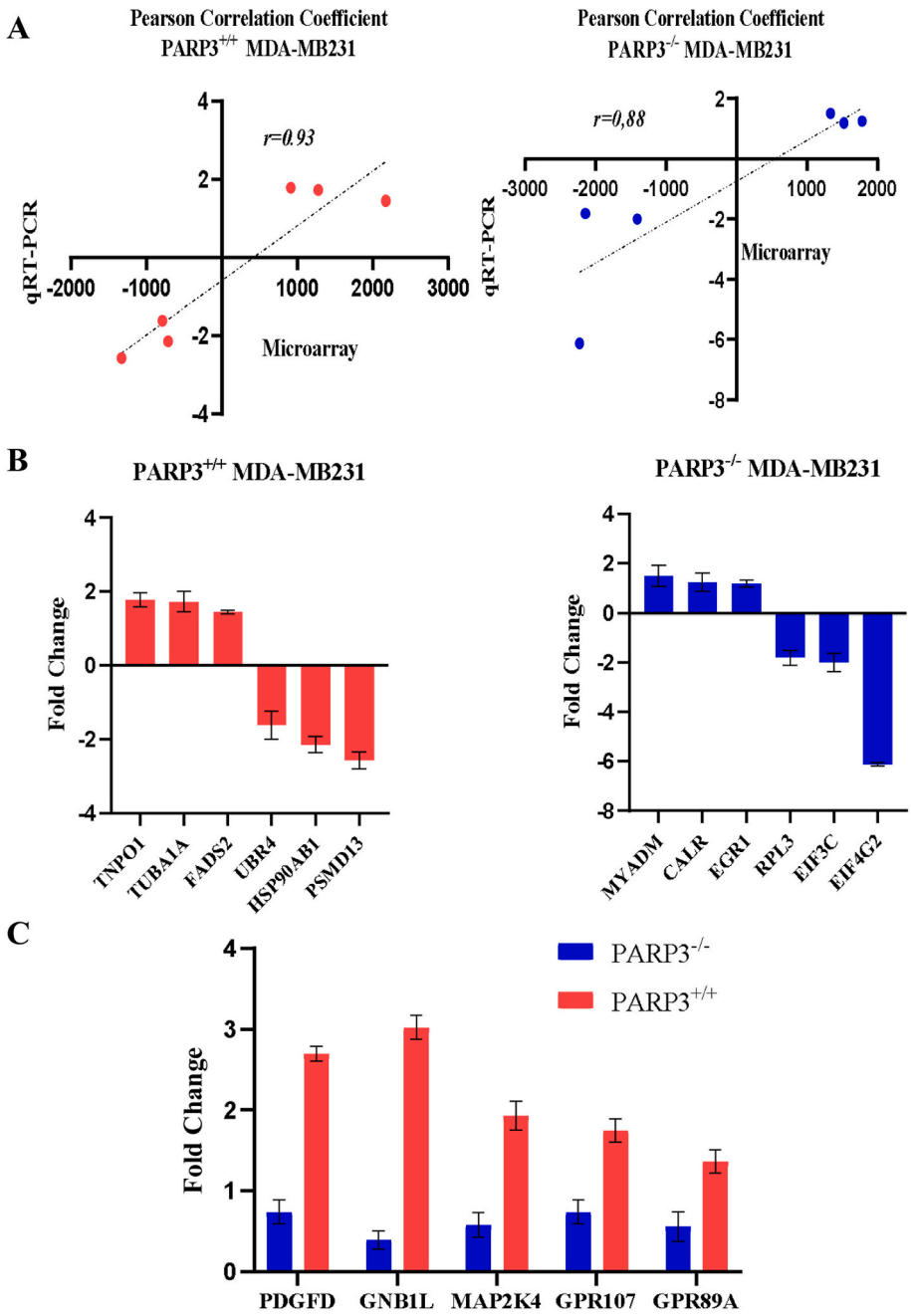

Fig. 5. A) Linear regressions and Pearson correlation coefficients for microarray and qRT-PCR data in *PARP3* wild-type and knockout MDA-MB-231 cells. B) Verification of the top three down- and up-regulated genes in these cells. C) Significant downregulation of *PDGFD, GNB1L, MAP2K4, GPR107*, and *GPR89A* genes in *PARP3* knockout MDA-MB-231 cells, with the opposite trend in the *PARP3* wild-type cells.

corresponding mechanisms by using microarray analyses. The other genes involved in BER were associated with various complex signaling pathways. Thus, blocking of distinct BER genes may result in various other molecular and cellular effects. For example, if NEIL3 has an impact on the PIK3K/AKT/mTOR signaling pathway, TDG is related to genes acting on cell cycle arrest, senescence, and death by mitotic alterations [55,56]. However, to obtain deeper information, comprehensive experimental analyses are required in the future.

The primary focus of our study was to demonstrate the alterations of neighbouring genes induced by the inhibition of *PARP3* in the response against cisplatin. The inhibition of *PARP3* plays a role the down-regulation of the mTOR signaling pathway, along with the restraint of TGFβ and reactive oxygen species (ROS)-driven epithelial-mesenchymal transition (EMT) [15,16]. Indeed, our data showed a downregulation of mTOR and apoptosis via *PARP3* blocking. Additionally, *PARP3* inhibition was found to suppress PDGF and G protein-coupled receptor (GPCR) signaling pathways, particularly affecting the expression of genes involved in the PDGF signaling pathway. The blocking of *TDG* and *NEIL3* were distinct consequences by affecting other signaling pathways. To understand the impact of *TGD* and *NEIL3* gene expression blocking, further experimental analyses are required.

Notably, PDGF assumes as modulator in the orchestration of diverse cellular processes, encompassing but not limited to cell proliferation, apoptotic regulation, cellular transformation, migration, invasion, angiogenesis, and the facilitation of metastasis [17]. Activation of PDGF fosters the survival and proliferation of cancer cells by engaging multiple oncogenic pathways such as phosphatidylinositol-3-kinase (PI3K/AKT), nuclear factor-κ B cells (NF-κB), Notch, extracellular

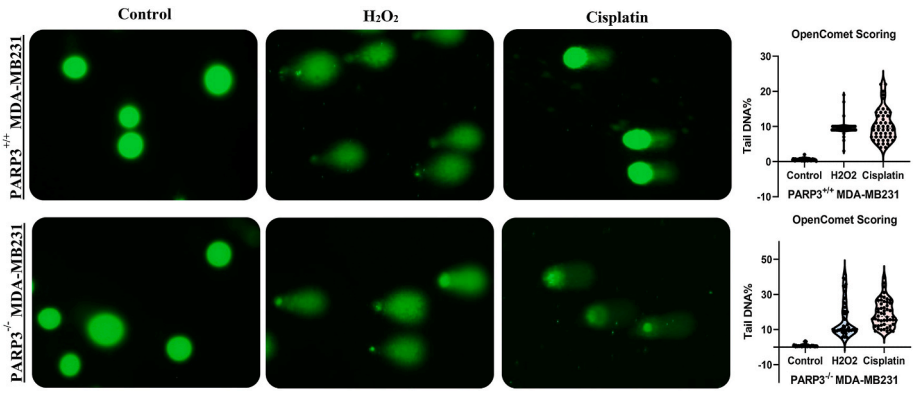

Fig. 6. Quantitative assessment of DNA damage using the alkaline comet assay, specifically single cell gel electrophoresis, following cisplatin exposure in *PARP3* wild-type and knockout MDA-MB-231 cells. The 'tail DNA%' parameter was quantified based on the analysis of 50 randomly selected cells, as illustrated in the accompanying violin plot.

signal-regulated kinase (ERK), mitogen-activated protein kinase (MAPK), and JAK-STAT [19,57–60].

The intricate interplay among various signaling pathways has a significant impact on protein-protein interactions. There exists a complex interplay among different signaling pathways, where the downregulation of one pathway exerts either a negative or positive influence on another. Illustrative examples on the relations between distinct signaling pathways have been published [61,62]. The efficient targeting to downregulate PI3K/AKT signaling revealed specific protein-protein interactions in the present of the inhibitor. The downregulation of PI3K/AKT has been considered as an alternative strategy to impede the growth of cancer cells by specific targeted ligands. Also, PDGF has a function in cancer progression by inducing proliferation, migration and cellular growth. The potential of PDGF as a therapeutic target is increasingly recognized. It is connected multiple signaling pathways responsible for cellular proliferation and growth. G protein-coupled receptors (GPCRs) is one of signal pathway affected by PDGF. In our studies, PDGF and GPCRs were downregulated through blocking of *PARP3* in breast cancer. Consequently, there are positive correlation between GPCRs, PDGF signaling pathways, and blocked *PARP3* expression. The development of potential ligands targeting PDGF is anticipated to inhibit cell proliferation by modulating the signaling pathways mentioned above.

In breast cancer, several studies showed the overexpression of PDGF as adverse prognostic factor [63,64]. Consequently, extensive research has focused on PDGF as a potential therapeutic target to combat cancer progression, as Its receptor and ligand play significant roles in drug resistance and oncogenesis [65,66]. Inhibition of PDGF, either directly or indirectly, holds promise as an approach in cancer treatment [67]. Our pathway analysis revealed that *PARP3* inhibition had a discernible impact on downregulating the PDGF signaling pathway.

Also, PDGF can be induced via GPCRs [68]. GPCRs are another modulators in tumor growth, angiogenesis, and metastasis, underscoring their significance as key players in cancer progression [69]. The upregulation of GPCR has profound effects on cancer-related signaling pathways, including AKT/mTOR, MAPKs, and the Hippo signaling pathway, which are intimately involved in cellular processes contributing to malignancy [70]. Therefore, comprehending the functional implications of GPCR in cancer drug treatment is of utmost importance in optimizing pharmacological strategies and identifying potential therapeutic targets [22]. In line with this, our study supports the proposition that *PARP3* knockdown, in the presence of cisplatin, affects GPCRs. We observed a lower function of GPCRs in *PARP3*$^{-/-}$ MDA-MB231 cells upon cisplatin exposure.

This was supported by robust evidence obtained through q-PCR verification, demonstrating the indirect influence of *PARP3* inhibition on afore-mentioned signal pathways involved in cancer progression. Notably, a pronounced upregulation was observed in the expression levels of *PDGFD, GNB1L, MAP2K4, GPR107*, and *GPR89A* genes if *PARP3* was present, as illustrated in Fig. 5C. In contrast, MDA-MB-231 breast cancer cells with the presence of *PARP3* inhibition exhibited a downregulation of these specific genes. This result indicates that knockout of *PARP3* suppressed the growth of MDA-MB-231 and increased cisplatin sensitivity. Moreover, less cisplatin concentration led to higher DNA damage in the *PARP3*$^{-/-}$ MDA-MB-231, which increased treatment efficiency at less side effects.

In conclusion, we demonstrated synthetic lethal interaction between GPCR, PDGF signaling pathways, and gene silencing of *PARP3*. In the cisplatin resistance, *PARP3* could be a promising target of a precision medicine approach. The combination of *PARP3* gene silencing and cisplatin drug may be a treatment method with fewer side effects by using lower doses of cisplatin concentration.

CRediT authorship contribution statement

Ayşegül Varol: Writing – review & editing, Writing – original draft, Validation, Software, Methodology, Investigation, Data curation, Conceptualization. **Sabine M. Klauck:** Writing – review & editing, Software, Methodology, Investigation, Data curation, Conceptualization. **Françoise Dantzer:** Methodology, Investigation, Conceptualization. **Thomas Efferth:** Writing – review & editing, Supervision, Project administration, Conceptualization.

Declaration of competing interest

The authors declare the following financial interests/personal relationships which may be considered as potential competing interests: Aysegul VAROL reports financial support was provided by Turkish Government (National Education Scholarship). If there are other authors, they declare that they have no known competing financial interests or personal relationships that could have appeared to influence the work reported in this paper.

Data availability

No data was used for the research described in the article.

Acknowledgement

We gratefully acknowledge the Microarray Unit of the Genomics and Proteomics Core Facility, German Cancer Research Center (DKFZ) Heidelberg, for providing excellent Expression Profiling service. A.V. is grateful for a stipend provided by the Turkish Government (National Education Scholarship).

Appendix A. Supplementary data

Supplementary data to this article can be found online at https://doi.org/10.1016/j.cbi.2024.111094.

References

[1] C.J. Norbury, I.D. Hickson, Cellular responses to DNA damage, Annu. Rev. Pharmacol. Toxicol. 41 (1) (2001) 367–401.
[2] G.-M. Li, Mechanisms and functions of DNA mismatch repair, Cell Res. 18 (1) (2008) 85–98.
[3] N. Chatterjee, G.C. Walker, Mechanisms of DNA damage, repair, and mutagenesis, Environ. Mol. Mutagen. 58 (5) (2017) 235–263.
[4] Y. Khazaei Monfared, et al., DNA damage by radiopharmaceuticals and mechanisms of cellular repair, Pharmaceutics 15 (12) (2023) 2761.
[5] L. Amable, Cisplatin resistance and opportunities for precision medicine, Pharmacol. Res. 106 (2016) 27–36.
[6] J. Liu, et al., Genetic polymorphisms of DNA repair pathways in sporadic colorectal carcinogenesis, J. Cancer 10 (6) (2019) 1417.
[7] H.E. Krokan, M. Bjørås, Base excision repair, Cold Spring Harbor Perspect. Biol. 5 (4) (2013) a012583.
[8] P. Fortini, et al., The base excision repair: mechanisms and its relevance for cancer susceptibility, Biochimie 85 (11) (2003) 1053–1071.
[9] U. Sattler, et al., Long-patch DNA repair synthesis during base excision repair in mammalian cells, EMBO Rep. 4 (4) (2003) 363–367.
[10] A. Gembka, et al., The checkpoint clamp, Rad9-Rad1-Hus1 complex, preferentially stimulates the activity of apurinic/apyrimidinic endonuclease 1 and DNA polymerase β in long patch base excision repair, Nucleic Acids Res. 35 (8) (2007) 2596–2608.
[11] S. O'Grady, et al., The role of DNA repair pathways in cisplatin resistant lung cancer, Cancer Treat Rev. 40 (10) (2014) 1161–1170.
[12] E. Belousova, A. Ishchenko, O. Lavrik, Dna is a new target of Parp3, Sci. Rep. 8 (1) (2018) 1–12.
[13] J.M. Rodriguez-Vargas, L. Nguekeu-Zebaze, F. Dantzer, PARP3 comes to light as a prime target in cancer therapy, Cell Cycle 18 (12) (2019) 1295–1301.
[14] H.L. Ko, E.C. Ren, Functional aspects of PARP1 in DNA repair and transcription, Biomolecules 2 (4) (2012) 524–548.
[15] O. Karicheva, et al., PARP3 controls TGFβ and ROS driven epithelial-to-mesenchymal transition and stemness by stimulating a TG2-Snail-E-cadherin axis, Oncotarget 7 (39) (2016) 64109.
[16] C. Beck, et al., PARP3, a new therapeutic target to alter Rictor/mTORC2 signaling and tumor progression in BRCA1-associated cancers, Cell Death Differ. 26 (9) (2019) 1615–1630.
[17] Z. Wang, et al., Emerging roles of PDGF-D signaling pathway in tumor development and progression, Biochim. Biophys. Acta Rev. Canc 1806 (1) (2010) 122–130.
[18] Z. Wang, et al., PDGF-D signaling: a novel target in cancer therapy, Curr. Drug Targets 10 (1) (2009) 38–41.
[19] Z. Wang, et al., Down-regulation of platelet-derived growth factor-D inhibits cell growth and angiogenesis through inactivation of Notch-1 and nuclear factor-κB signaling, Cancer Res. 67 (23) (2007) 11377–11385.
[20] C.-H. Heldin, Targeting the PDGF signaling pathway in tumor treatment, Cell Commun. Signal. 11 (2013) 1–18.
[21] R. Bar-Shavit, et al., G protein-coupled receptors in cancer, Int. J. Mol. Sci. 17 (8) (2016) 1320.
[22] Y. Liu, et al., G protein-coupled receptors as promising cancer targets, Cancer Lett. 376 (2) (2016) 226–239.
[23] E. Cerami, et al., The cBio cancer genomics portal: an open platform for exploring multidimensional cancer genomics data, Cancer Discov. 2 (5) (2012) 401–404.
[24] J. Gao, et al., Integrative analysis of complex cancer genomics and clinical profiles using the cBioPortal, Sci. Signal. 6 (269) (2013) pl1-pl1.
[25] J. O'brien, et al., Investigation of the Alamar Blue (resazurin) fluorescent dye for the assessment of mammalian cell cytotoxicity, Eur. J. Biochem. 267 (17) (2000) 5421–5426.
[26] K.J. Livak, T.D. Schmittgen, Analysis of relative gene expression data using real-time quantitative PCR and the 2− ΔΔCT method, Methods 25 (4) (2001) 402–408.
[27] B.M. Gyori, et al., OpenComet: an automated tool for comet assay image analysis, Redox Biol. 2 (2014) 457–465.
[28] G. Housman, et al., Drug resistance in cancer: an overview, Cancers 6 (3) (2014) 1769–1792.
[29] S. Tanida, et al., Mechanisms of cisplatin-induced apoptosis and of cisplatin sensitivity: potential of BIN1 to act as a potent predictor of cisplatin sensitivity in gastric cancer treatment, Int. J. Surg. Oncol. (2012) 2012.
[30] S.-H. Chen, J.-Y. Chang, New insights into mechanisms of cisplatin resistance: from tumor cell to microenvironment, Int. J. Mol. Sci. 20 (17) (2019) 4136.
[31] Q. Wang, P. Li, W. Wu, A systematic analysis of immune genes and overall survival in cancer patients, BMC Cancer 19 (2019) 1–9.
[32] D. Lebwohl, et al., Progression-Free survival: gaining on overall survival as a gold standard and AcceleratingDrug development, Cancer J. 15 (5) (2009) 386–394.
[33] R.J. Motzer, et al., Overall survival and updated results for sunitinib compared with interferon alfa in patients with metastatic renal cell carcinoma, J. Clin. Oncol. 27 (22) (2009) 3584.
[34] T. Adachi, et al., Oxaliplatin and molecular-targeted drug therapies improved the overall survival in colorectal cancer patients with synchronous peritoneal carcinomatosis undergoing incomplete cytoreductive surgery, Surg. Today 45 (2015) 986–992.
[35] R. Dienstmann, et al., Prediction of overall survival in stage II and III colon cancer beyond TNM system: a retrospective, pooled biomarker study, Ann. Oncol. 28 (5) (2017) 1023–1031.
[36] S.J. Cohen, et al., Relationship of Circulating Tumor Cells to Tumor Response, Progression-free Survival, and Overall Survival in Patients with Metastatic Colorectal Cancer, 2008.
[37] V. Gupta, et al., Survival prediction tools for esophageal and gastroesophageal junction cancer: a systematic review, J. Thorac. Cardiovasc. Surg. 156 (2) (2018) 847–856.
[38] L. Liu, et al., Breast cancer survival prediction using seven prognostic biomarker genes, Oncol. Lett. 18 (3) (2019) 2907–2916.
[39] H. Huang, Q. Hua, NEIL3 mediates lung cancer progression and modulates PI3K/AKT/mTOR signaling: a potential therapeutic target, Int. J. Genomics (2022) 2022.
[40] J.-J. Quan, J.-N. Song, J.-Q. Qu, PARP3 interacts with FoxM1 to confer glioblastoma cell radioresistance, Tumor Biol. 36 (2015) 8617–8624.
[41] G. Wang, et al., Comprehensive analysis of the prognostic value and biological function of TDG in hepatocellular carcinoma, Cell Cycle 22 (12) (2023) 1478–1495.
[42] Z. Song, et al., Poly (ADP-ribose) polymerase-3 overexpression is associated with poor prognosis in patients with breast cancer following chemotherapy, Oncol. Lett. 16 (5) (2018) 5621–5630.
[43] M.E. Dolan, Inhibition of DNA repair as a means of increasing the antitumor activity of DNA reactive agents, Adv. Drug Deliv. Rev. 26 (2–3) (1997) 105–118.
[44] C.G. Broustas, H.B. Lieberman, DNA damage response genes and the development of cancer metastasis, Radiat. Res. 181 (2) (2014) 111–130.
[45] A. Kumar, et al., Reduced expression of DNA repair genes (XRCC1, XPD, and OGG1) in squamous cell carcinoma of head and neck in North India, Tumor Biol. 33 (2012) 111–119.
[46] M. Petrosino, et al., Analysis and interpretation of the impact of missense variants in cancer, Int. J. Mol. Sci. 22 (11) (2021) 5416.
[47] V. Gotea, et al., The functional relevance of somatic synonymous mutations in melanoma and other cancers, Pigment Cell Melanoma Res. 28 (6) (2015) 673–684.
[48] R.R. Haraksingh, M.P. Snyder, Impacts of variation in the human genome on gene regulation, J. Mol. Biol. 425 (21) (2013) 3970–3977.
[49] B.S. Strauss, Frameshift mutation, microsatellites and mismatch repair, Mutat. Res. Rev. Mutat. Res. 437 (3) (1999) 195–203.
[50] Y. Mantri, S.J. Lippard, M.-H. Baik, Bifunctional binding of cisplatin to DNA: why does cisplatin form 1, 2-intrastrand cross-links with AG but not with GA? J. Am. Chem. Soc. 129 (16) (2007) 5023–5030.
[51] S. Rezaei, et al., Investigation on the effect of fluorescence quenching of calf thymus DNA by piperine: caspase activation in the human breast cancer cell line studies, DNA Cell Biol. 43 (1) (2024) 26–38.
[52] P.B. Tchounwou, et al., Advances in our understanding of the molecular mechanisms of action of cisplatin in cancer therapy, J. Exp. Pharmacol. (2021) 303–328.
[53] S.J. Shukla, et al., Susceptibility loci involved in cisplatin-induced cytotoxicity and apoptosis, Pharmacogenetics Genom. 18 (3) (2008) 253–262.
[54] M.A. Farooq, et al., Recent progress in nanotechnology-based novel drug delivery systems in designing of cisplatin for cancer therapy: an overview, Artif. Cell Nanomed. Biotechnol. 47 (1) (2019) 1674–1692.
[55] W. Wang, et al., NEIL3 contributes toward the carcinogenesis of liver cancer and regulates PI3K/Akt/mTOR signaling, Exp. Ther. Med. 22 (4) (2021) 1–11.
[56] P. Mancuso, et al., Thymine DNA glycosylase as a novel target for melanoma, Oncogene 38 (19) (2019) 3710–3728.
[57] D. Kong, et al., Mammalian target of rapamycin repression by 3, 3′-diindolylmethane inhibits invasion and angiogenesis in platelet-derived growth factor-D–overexpressing PC3 cells, Cancer Res. 68 (6) (2008) 1927–1934.
[58] M.-L. Vignais, et al., Platelet-derived growth factor induces phosphorylation of multiple JAK family kinases and STAT proteins, Mol. Cell Biol. 16 (4) (1996) 1759–1769.
[59] M.-L. Vignais, M. Gilman, Distinct mechanisms of activation of Stat1 and Stat3 by platelet-derived growth factor receptor in a cell-free system, Mol. Cell Biol. 19 (5) (1999) 3727–3735.
[60] N.A. Lokker, et al., Platelet-derived growth factor (PDGF) autocrine signaling regulates survival and mitogenic pathways in glioblastoma cells: evidence that the novel PDGF-C and PDGF-D ligands may play a role in the development of brain tumors, Cancer Res. 62 (13) (2002) 3729–3735.
[61] M. Kaffash, et al., Spectroscopy and molecular simulation on the interaction of Nano-Kaempferol prepared by oil-in-water with two carrier proteins: an investigation of protein–protein interaction, Spectrochim. Acta Mol. Biomol. Spectrosc. 309 (2024) 123815.
[62] Z. Malek-Esfandiari, et al., Molecular dynamics and multi-spectroscopic of the interaction behavior between bladder cancer cells and calf thymus DNA with rebeccamycin: apoptosis through the down regulation of PI3K/AKT signaling pathway, J. Fluoresc. 33 (4) (2023) 1537–1557.
[63] L. Seymour, W. Bezwoda, Positive immunostaining for platelet derived growth factor (PDGF) is an adverse prognostic factor in patients with advanced breast cancer, Breast Cancer Res. Treat. 32 (1994) 229–233.
[64] I. Carvalho, et al., Overexpression of platelet-derived growth factor receptor α in breast cancer is associated with tumour progression, Breast Cancer Res. 7 (5) (2005) 1–8.
[65] K. Pietras, et al., PDGF receptors as cancer drug targets, Cancer Cell 3 (5) (2003) 439–443.

[66] M.T. Weigel, et al., Preclinical and clinical studies of estrogen deprivation support the PDGF/Abl pathway as a novel therapeutic target for overcoming endocrine resistance in breast cancer, Breast Cancer Res. 14 (3) (2012) 1–15.
[67] P. Pandey, et al., New insights about the PDGF/PDGFR signaling pathway as a promising target to develop cancer therapeutic strategies, Biomed. Pharmacother. 161 (2023) 114491.
[68] J.-B. Demoulin, A. Essaghir, PDGF receptor signaling networks in normal and cancer cells, Cytokine Growth Factor Rev. 25 (3) (2014) 273–283.
[69] R.T. Dorsam, J.S. Gutkind, G-protein-coupled receptors and cancer, Nat. Rev. Cancer 7 (2) (2007) 79–94.
[70] M. O'Hayre, M.S. Degese, J.S. Gutkind, Novel insights into G protein and G protein-coupled receptor signaling in cancer, Curr. Opin. Cell Biol. 27 (2014) 126–135.